Peculiar properties in the behavior of energetic charged particles and in total electron content variations during geomagnetic storm on March 17, 2013

O. V. Dudnik, Y. M. Zanimonskiy, Institute of Radio Astronomy, National Academy of Sciences of Ukraine (IRA NASU); dudnik @rian.kharkov.ua

Abstract

During the main phase of the geomagnetic storm depletion of Van Allen radiation belts take place. At the recovery phase, acceleration and intensification of particle fluxes play a predominant role. The gap between the inner and outer belts is being filled frequently by electrons, the energy spectra of which much wider than in a more steady inner radiation belt. During geomagnetic storms, there are also significant fluctuations of the electron density in the Earth's plasmasphere. One of the consequences of such fluctuations is variations of the total electron content, which is being determined from the data of the Global Navigation Satellite System.

In the present study, we analyze dynamics of high-energy electrons based on the data taken from the NOAA patrol satellite and analyze maps of total electron content variations above Central Europe during the geomagnetic storm on March 17, 2013. We demonstrate that coronal mass ejection caused significant variations of charged particle fluxes intensity in the inner layers of the magnetosphere. We show that motion of the southern boundary of total electron content variations in the Northern hemisphere to the southern direction is being coincided with changes in the location of the southern boundary of the penetration onto heights of low-orbiting satellites of electrons with energies of few tens of keV during the main phase of the geomagnetic storm. We assume medium-scaled variations of total electron content at the middle latitudes can be associated with sporadic microbursts of high-energy electrons under Van Allen radiation belts and in the gap between inner and outer belts.

1. INTRODUCTION

Magnetic storms in the Earth's magnetosphere are accompanied by variations of electron concentration in the ionosphere and plasmasphere. It is known that several processes in the magnetosphere-ionosphere-thermosphere system can induce intense changes in the global distribution of plasma densities. Such changes are noticeable during disturbed magnetosphere in which ionospheric F-layer densities can increase, or decrease, by a factor of 5-10. Electric fields can lead to increases of the density by raising the layer height; they modify the fountain effect at the equator and transport the crests of the equatorial anomaly poleward (Mannucci et al. 2005). Expanded auroral oval generally occurs during geomagnetic storms (Heelis and Mohapatra 2009). Heelis et al. (2009) demonstrated that this auroral oval was sufficient to create dayside Total Electron Content (TEC) enhancements amplified by a factor of 2 or more. Besides, plasma instabilities can also create pronounced redistributions of the mid-latitude plasma by the generation of Medium-Scale Traveling Ionospheric Disturbances (MSTIDs) (Perkins 1973).

Valladares et al. (2017) have shown that during two moderate storms the plasma density within the Storm Enhanced Densities (SEDs) does not originate from the equatorial anomaly as the anomaly crests do not move poleward of 20° magnetic latitude. They also indicated that the TEC along the SED forms all at once and is not transported from further eastward locations. During geomagnetic storms, the SEDs are observed to move equatorward and are associated with an equatorward expansion of the auroral oval (Valladares et al. 2017). Authors observed a second region containing enhanced TEC at mid-latitudes during both storms. This region of enhanced TEC merges with the SED developing finger-type structures that appear to be associated with a large-scale plasma instability.

Unexpected localized TEC enhancement (LTE) in the form of two plumes centered southward of Africa, observed slightly after noontime during a moderate geomagnetic storm of 15 August 2015 (Edemskiy et al.

2018). A similar LTE does not occur in the Northern Hemisphere, authors conclude that it is a Southern Hemisphere phenomenon. Its origin is not understood yet.

At the same time, during the main phase of the storm, the processes of high energy electron diffusion in radiation belts are intensified finally to leading to their further precipitation into the atmosphere. Typical radiation belt pattern amongst the strongest coronal mass ejection (CME)-driven storms is one where the initial interplanetary shock wave, which moves ahead of the driving interplanetary CME itself, greatly compresses and distorts the Earth's magnetosphere. Baker et al. (2016) shown that this magnetospheric compression leads to profound relativistic electron losses due to magnetopause shadowing and resulting strong radial gradients.

The initial phase of most geomagnetic storms is characterized by a precipitous fall in the flux of electrons detected by weather satellites — often by many orders of magnitude in just a few hours. The mechanism that causes these "flux dropouts" has never been clear (Hudson 2012). Turner et al. (2012) shown that wave-induced precipitation into the atmosphere cannot account for the initial flux dropout, as the precipitation signal observed by the POES satellites occurred a day after the event, during the recovery phase of the storm when the electron flux was increasing. Authors suggested that the electrons are lost outwards towards the magnetopause — the outer boundary of the Earth's magnetosphere. They based on the THEMIS satellites observations that revealed a significant increase in the ultralow-frequency plasma waves during the dropout phase, contributing to outward radial transport and loss to the magnetopause, as the magnetopause moves inward with increased solar wind pressure.

In some cases, a gap between the inner and outer Van Allen electron radiation belts is filled by enhanced energetic particles (Hudson et al. 2008) that may affect on the spatial distribution of the TEC both: in plasmasphere and in the ionosphere. Both processes, most likely, are closely related to each other: non-stationary streams of high-energy particles with small pitch-angles at the altitudes of low Earth-orbiting satellites can affect the spatial distributions of TEC. Suvorova et al. (2013) demonstrated that during magnetic storms, energetic (~30 keV) electrons drift fast radially from the inner radiation belt to ionospheric altitudes located within the night side sector. Then, quasi-trapped electrons, drifting azimuthally eastward, exhaust their energy during the ionization of atmospheric gases and produce abundant ionization within the low- and mid-latitude ionosphere.

Suvorova et al. (2014) based on the data analysis from low-orbiting POES, DMSP and GOSAT satellites concluded that the intense fluxes of energetic electrons penetrating to ionospheric heights produce an additional ionization of the order of 10 TECU at low to middle latitudes. The ionization can occur in a wide range of local times and longitudes. Besides, the effects of ionizing particles become evident during the recovery phase when other storm-time mechanisms can be ruled out.

In this work, we analyze dynamics of high energy electrons by using the database from the NOAA / POES patrol satellite and analyze maps of TEC variations over Central Europe during the geomagnetic storm on March 17, 2013.

2. EXPERIMENTAL DATA

Electron fluxes were recorded in several integral energy ranges from two mutually perpendicular directions by the MEPED (Medium Energy Proton Electron Detector) instrument, a part of the SEM-2 scientific equipment (Space Environment Monitor-2). The SEM-2 equipment, by-turn, is installed on board the low orbit spacecraft NOAA-15. The NOAA-15 is one of NOAA / POES / MetOp satellites, each of which flies around the Earth with a period of t_{cir} = 102 min. and with a quasi-circular solar-synchronous orbit at the altitude $h_{POES} \approx 850$ km. One of the two telescopes of the MEPED device captures particle streams from the "anti-Earth" direction, i.e. the axis of the solid angle of this telescope, into which the particles fall down, coincides with the line connecting the spacecraft with the center of the Earth. The second telescope registers particle fluxes from the horizontal direction, which has an inverse direction to the satellite's velocity vector. The electron fluxes are being measured in four energy ranges: E1 ($E_e > 40$ keV), E2 ($E_e > 130$ keV), E3 ($E_e > 287$ keV), and E4 ($E_e > 612$ keV).

Maps of TEC variations were constructed as results of processing the signals received from the Global Navigation Satellite System (GNSS) satellites located near zenith (with an elevation angle more than of 70°). Data of about 600 terrestrial dual-frequency receivers were used. Each map with a spatial resolution of about 50 km has been calculated using a special algorithm of de-trending and with the further usage of the deviations of TEC from smoothed regional values (Nykiel et al. 2017). Temporal interval between sequential maps is equal to 30 s, a step of the uniform grid by latitude and longitude is equal to 0.1°. Realization of the possibility to measure TEC in accordance with its direct determination eliminated a necessity to introduce model representations about the ionosphere as a thin screen at a certain height.

3. GEOPHYSICAL CONDITIONS DURING THE STORM OF MARCH 17, 2013

A long-drawn solar flare during time interval $\Delta t_2 \approx$ 06h:46m – 09h:35m UTC with a maximum at t_{max} = 07h:58m UTC on March 15, 2013, of M1.1 class was the source of enhanced fluxes of high energy particles of different species, and of Coronal Mass Ejection (CME). The front of CME shock, which is being characterized by a sharp and simultaneous increase of

the solar wind (SW) velocity from $V_{SW1} \approx 450$ km/s to $V_{SW2} \approx 650$ km/s, and of SW density from $\rho_1 \approx 4$ part/cm^3 to $\rho_2 \approx 10$-20 part/cm^3, and of temperature from $T_1 \approx 1 \times 10^5$°K to $T_2 \approx 7 \times 10^5$°K, generated a strong geomagnetic storm with a sudden commencement SC at $t_{SC} \approx$ 06h:02m UTC and with a prolonged main phase which was lasting from $t_{mf1} \sim$ 10h:30m UTC to $t_{mf2} \sim$ 20h:30m UTC with a maximum value of $D_{st} = -132$ nT. Due to geoefficiency of the solar flare, on March 17 a strong compression of the magnetosphere has been observed: the position of bow shock decreased from $X_1 \approx 15$ R_e to $X_2 \approx 8$ R_e for a short time $\Delta t_3 \approx$ 05h:06m – 08h:24m UTC (Fig. 1a). This served as the development of a prolonged geomagnetic storm (Fig. 1b).

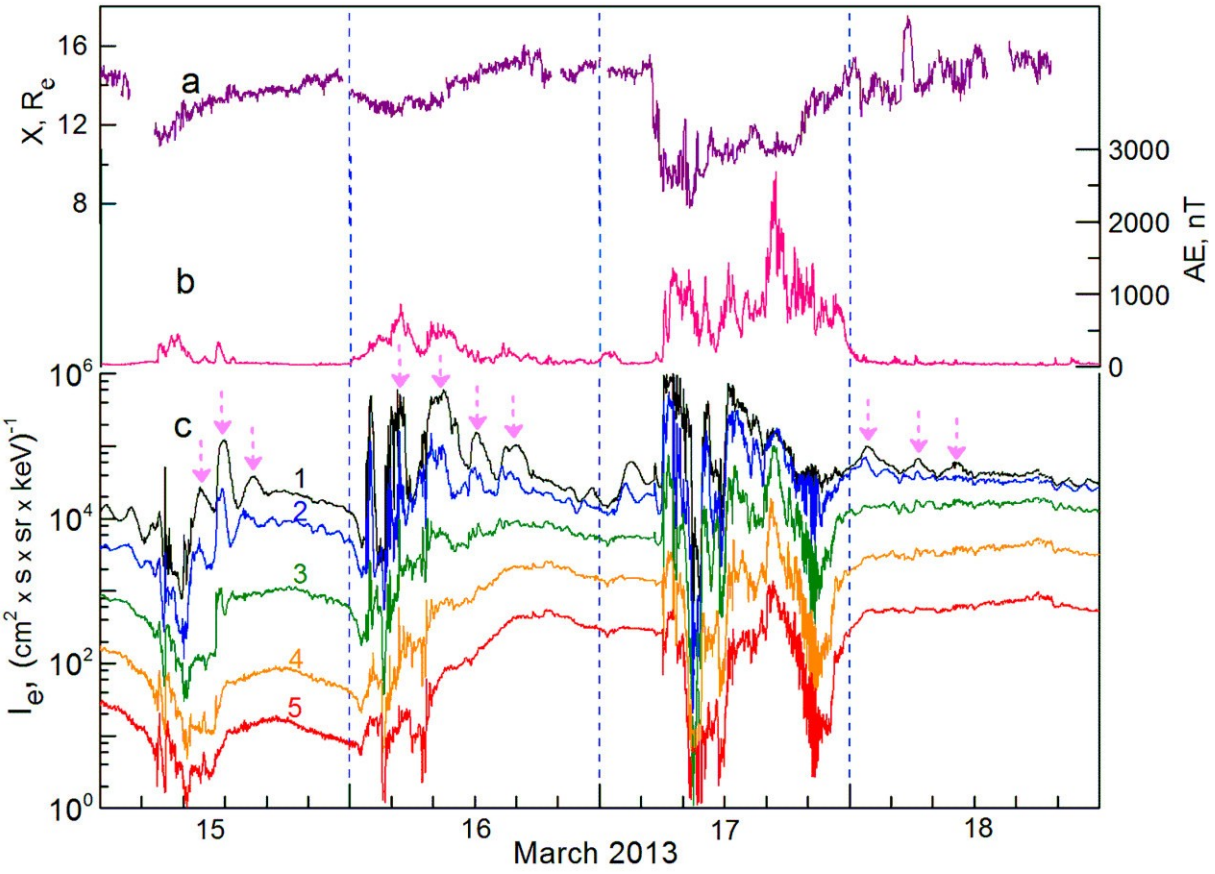

Figure 1. 1-minute's data of* a*: magnetosphere bow shock nose location in the ecliptic plane;* b*: AE-index;* c*: spectral density of electron fluxes from the "anti-Earth" direction at geostationary orbit by the data of GOES-13 in 5 energy ranges:* 1 *–* $E_e > 40$ *keV,* 2 *–* $E_e > 75$ *keV,* 3 *–* $E_e > 150$ *keV,* 4 *–* $E_e > 275$ *keV,* 5 *–* $E_e > 475$ *keV for the period from March, 15 to March, 18 of 2013. Time scale is in UTC.

The increase of electron, proton and ion fluxes in the near-Earth space with an insignificant count rate growth was recorded in the second half of March 15, and with a more significant gradient of growth at the end of March 16, according to the data of the ACE and WIND satellites at the Lagrangian point L1. Particle fluxes in the interplanetary space reached their maximum in the first half of March 17. They served as a source of significant variations of the electron fluxes at the outer edge of the Van Allen outer belt according to measurements at GOES geostationary satellites. In addition, the processes of pitch-angle diffusion increased with a decrease of trapped particles content and with simultaneous replenishment of the belt due to injection of particles from the interplanetary space that was accelerated at the front of CME.

In Fig. 1c vertical arrows indicate the peaks of the "drift echo" of low energy ($E_e > 40$ keV) electrons and of intermediate energy electrons. The "drift echo" occurs as a result of injection processes of narrowly directed particle beams that are of impulse nature from the interplanetary magnetic field, of the capture of the particle beam parts by the Earth's magnetic field, followed by multiple azimuths drift around the Earth with returning to initial primary injection zone. Fig. 1c also demonstrates that the energy spectrum of electrons injected from the outside has a falling down character, the upper energy limit of the particles does not exceed the value $E_e = 0.5$ MeV.

4. DYNAMICS OF ENERGETIC ELECTRONS THE NORTHERN HEMISPHERE

Enhanced fluxes of subrelativistic and relativistic electrons were detected at the end of March, 16 and during March, 17 according to the data of the NOAA-15 satellite at the Northern hemisphere at high latitudes in the region of opened force lines of the geomagnetic field. Low and medium energy electrons have got into the loss cone in the spatial region of the outer radiation belt in time the prolonged compression of the magnetosphere on March 16 and 17 (Fig. 1a) and of the growth of AE-index (Fig. 1b). The increase of the particle flux in the loss cone in the inner radiation belt zone was observed only in short intervals of pulse growth of SW velocity and density and in the main phase of the storm.

Penetration of flare electrons with energies E_e > 40 keV from the interplanetary space onto low magnetosphere heights in the Northern hemisphere was recorded by the POES satellite at the end of March 16, and during March 17 at latitudes from 81° N up to latitudes of the projection of the Van Allen outer radiation belt onto the Earth's surface (Fig. 2).

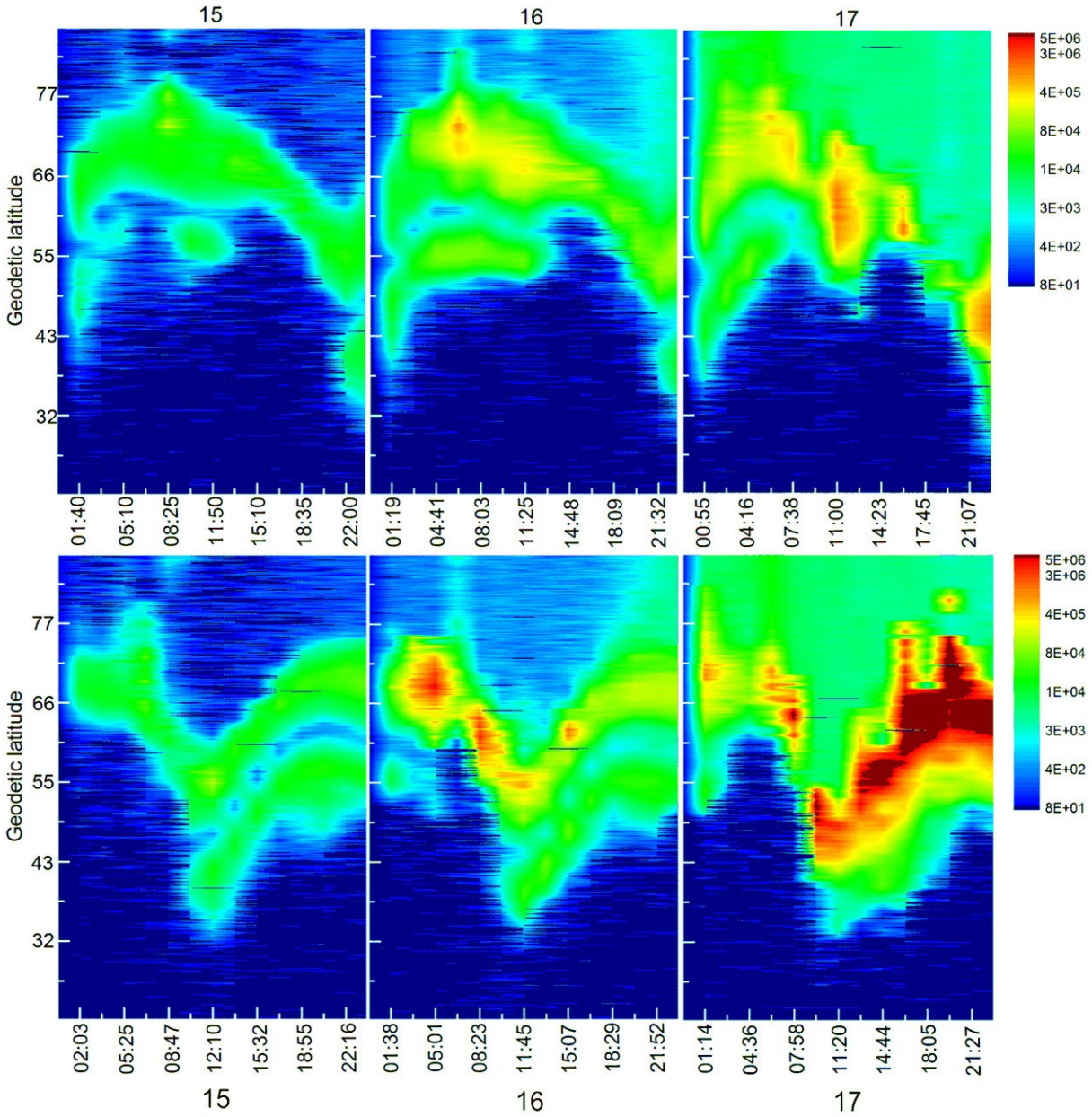

Figure 2. Dynamics of electron fluxes with energies E_e > 40 keV in the Northern hemisphere in the interval of latitudes 20° - 80° N during the period from 15 to 17 March 2013 according to MEPED / SEM-2 / POES data recorded from the horizontal direction at daytime (upper half) and in the pre-morning (bottom part) hours of local magnetic time. Electron fluxes in the form of a 64-level color scale are represented in units of particles / (cm² × s ster). The time scale is in UTC.

A significant part of particles immediately entered into the loss cone and was detected by sensors with view axis orienting in the direction of "anti-Earth" (Fig. 3). Injection of electrons onto outer belt region; accelerating processes and rapid radial diffusion of outer belt particles downward to the inner part of magnetosphere; disappearance of the gap between belts, sharp increase of pulsed precipitating fluxes in the pre-dawn hours occurred during the main phase of the geomagnetic storm (right figure of panel b, Fig. 2) with the start of injection at $\Delta t_4 \approx$ 06h:30m – 07h:30m UTC. Whilst in this temporal interval the lower boundary along the latitude of non-background quasi-trapped particle fluxes was observed at latitude $\varphi_1 \approx 52°$ N, then in the interval between $\Delta t_5 \approx$ 08h:08m – 09h:29m UTC this boundary shifted to $\varphi_2 \approx 40°$N, but in the time window from 11h:10m to 11h:30m UTC the lower boundary reached the minimum value of $\varphi_3 \approx 32°$N.

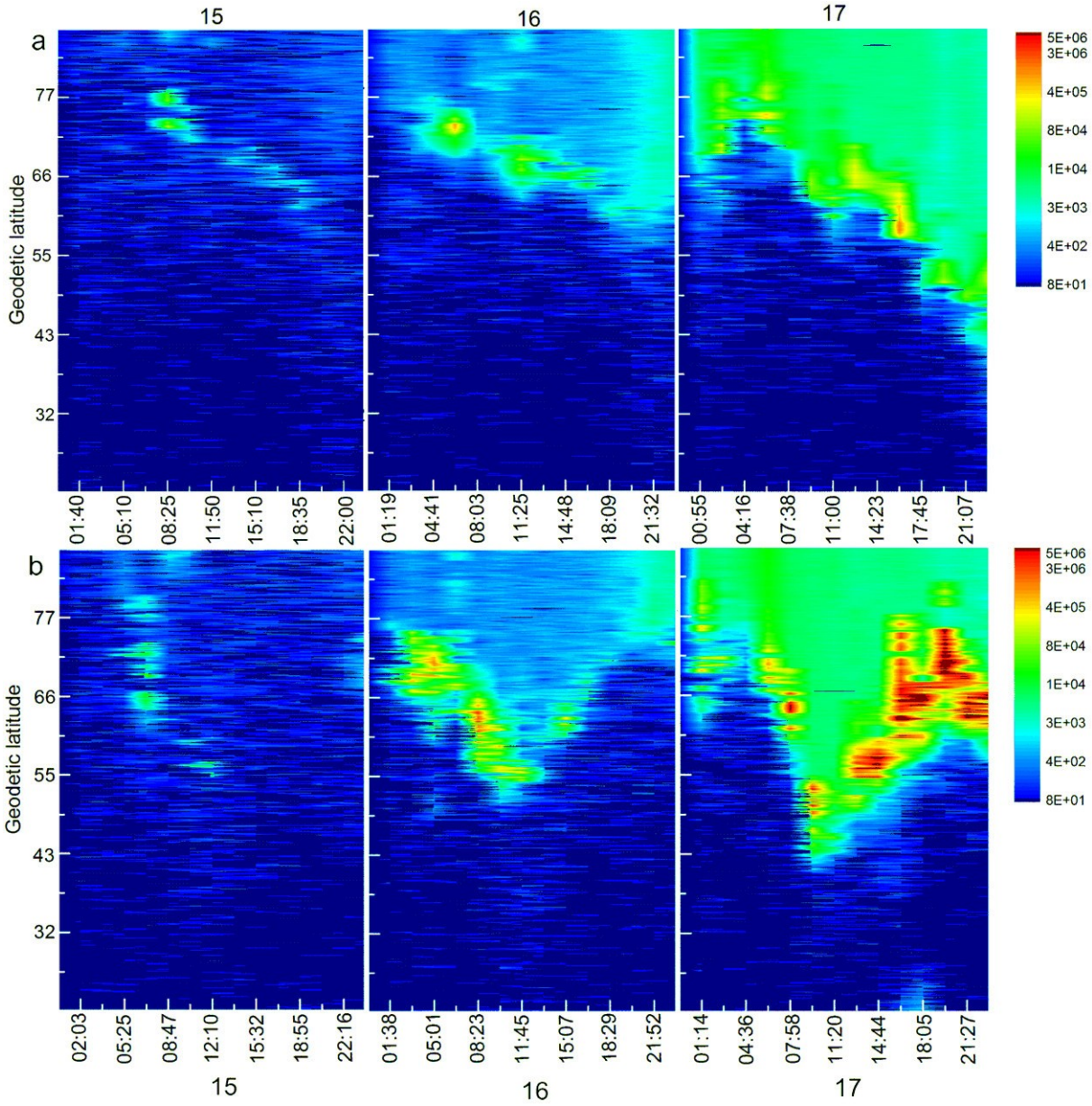

Figure 3. The same as on Figure 2, but for electrons that were recorded from "anti-Earth" direction

The southern latitude boundary of precipitating electrons that were measured from the "anti-Earth" direction has reached value $\varphi_4 \approx 42°$ N, and remained at this level within time interval $\Delta t_6 \approx$ 09h:30m – 11h:30m UTC on March 17, while on the previous day at a similar time window the lower boundary reached the minimum value of $\varphi_5 \approx 52°$N.

5. FEATURES OF TEC VARIATIONS OVER CENTRAL EUROPE IN MARCH 2013

The dependence of the level of TEC variations vs. latitude at different phases of the storm is revealed. The conditional boundary, to the north of which the level of variation substantially increases, passes near 52° N parallel to the isolines of the geomagnetic field (Fig. 4). The position of the boundary at the onset of the storm changes insignificantly within few hours.

Electrons in plasmasphere make a noticeable contribution to TEC along the line of sight "GNSS satellite-terrestrial receiver". Earlier tomographic studies using GNSS signals have shown that the plasmaspheric electrons are concentrated into finger-like structures extending from the upper ionosphere to a height of several thousand kilometers and having transverse dimensions from 200 to 400 km. At the bottom of these structures, located at ionospheric heights, the electron concentration is higher than in neighboring regions and smoothly decreases to an altitude of about ten thousand kilometers, gradually increasing at high altitudes (Yizengaw et al. 2005, Yizengaw et al. 2006).

On the TEC variations maps over Central Europe during this storm, the quasi-periodical formations have been detected existing during 2-3 hours. Their direction changes during the satellite flight in accordance with the change of its angular coordinates (Fig. 4).

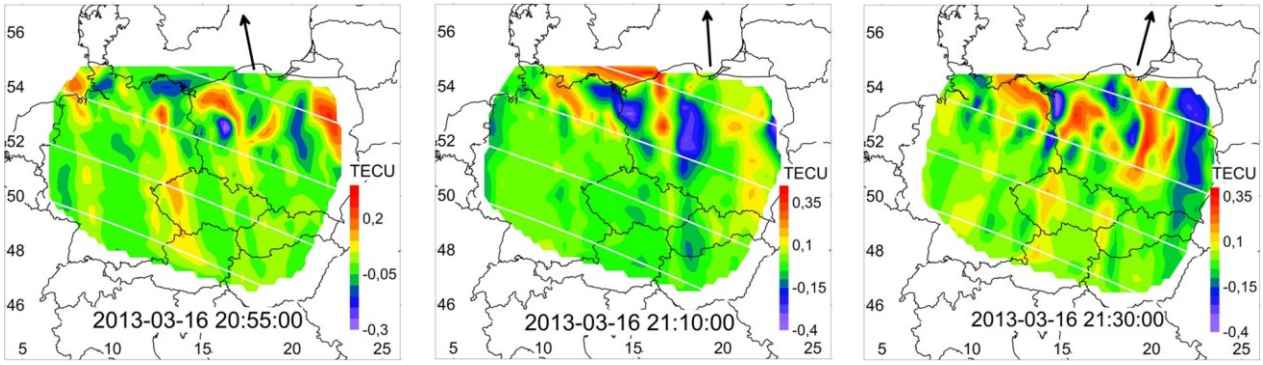

Figure 4. Maps of TEC variations over Central Europe before sudden commencement of the geomagnetic storm on March 17, 2013. Arrows indicate the projections of directions to GNSS satellite. In white color isolines of the geomagnetic field at ionospheric altitude are shown.

Magnitospheric finger-like structures of variable density, oriented along geomagnetic field lines, are being projected on the south part of maps in a form of the "tails" corresponding to increased electron concentration in the magnetosphere, and of the "heads" with a high concentration of electrons in the ionospheric plasma in the north part of the map.

We suppose that in high-altitude parts of the finger-like structures the signal of the GNSS satellite passes through the zone in which trapped and quasi-trapped electron fluxes are being concentrated near their mirror reflection points (Fig. 5). Accordingly, the increases of TEC in comparison with zones outside of structures, as well as the rotation of the „tail" on the map synchronized with the motion of the GNSS satellite are noticeable. In the bottom parts of finger-like structures resting upon the ionosphere, ionization of the residual atmosphere by high-energy electrons is observed. As a result, a large number of secondary electrons are produced that are manifested as an increase of TEC in regions of "heads". As far as the "heads" of structures are presumably formed at ionospheric heights their displacement along geographic coordinates was not noticed when the GNSS satellite moved. The jagged by intensities temporal profiles of high energy electron fluxes with energies of tens of keV recorded on the NOAA-15 spacecraft with a time resolution of 2 seconds can be as the reason for registration of "finger-like" structures in TEC.

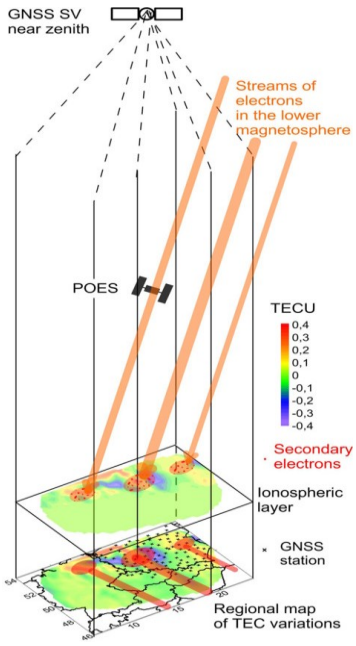

Figure 5. Model of the mapping of energetic electrons forming finger-like structures in the magnetosphere in the form of "tails" and secondary electrons in the form of "heads" on the map of TEC variations.

Visualization of electron density spatial distribution in the bottom part of the magnetosphere, demonstrated in this work, is like the results of tomographic studies. However, there is one significant difference. In our studies, the solutions of inverse tasks are not carried out and, accordingly, the minimum requirements are applied to the models used. These requirements constitute an independence of spatial-temporal distributions of the electron content in the ionosphere along horizontal, and in the magnetosphere along vertical. Requirements, accompanied by the provision of the presence of noticeable spatial variations of TEC, which are relatively stable in time scales of about dozen minutes, are realized in some phases of the geomagnetic storm.

It should also be noticed that the fundamental fact in this study is that the signals of high-orbiting GNSS satellites "shine through" the entire of the lower magnetosphere. Further work on the mapping of TEC disturbances, conducted continuously in monitoring mode, can provide new information on dynamic processes in the ionosphere and the lower magnetosphere.

6. CONCLUSIONS

The geo-effective solar flare on March 15, 2013, was a source of the geomagnetic storm that followed caused significant variations of particle fluxes intensity in the inner layers of the magnetosphere.

The motion of the southern boundary of TEC variations in the Northern hemisphere is being confirmed with changes in the location of the southern boundary of the penetration of electrons with energies of tens of keV onto heights of low-orbiting satellites during the main phase of the geomagnetic storm.

Medium-scaled variations of TEC at the middle latitudes can be associated with sporadic microbursts of high-energy electrons below Van Allen radiation belts and in the gap between inner and outer belts. Variations of TEC contain significant information on processes in the ionosphere and magnetosphere. Visualization of variations provides one more effective tool for retrieval of this information.

REFERENCES

Baker, D.N., Jaynes, A.N., Kanekal, S.G., Foster, J.C., Erickson, P.J., Fennell, J.F., Blake, J.B., Zhao, H., Li, X., Elkington, S.R., Henderson, M.G., Reeves, G.D., Spence, H.E., Kletzing, C.A., Wygant, J.R.:2016, Highly relativistic radiation belt electron acceleration,transport, and loss: Large solar storm events of March and June 2015, *Journal of Geophysical Research: Space Physics* **121**(7), 6647–6660.

Edemskiy, I., Lastovicka, J., Buresova, D., Habarulema, J.B., Nepomnyashchikh, I.:2018, Unexpected Southern Hemisphere ionospheric response to geomagnetic storm of 15 August 2015, *Annales Geophysicae* **36**(1): 71–79.

Heelis, R.A., and Mohapatra, S.:2009, Storm time signatures of the ionospheric zonal ion drift at middle latitudes, *Journal of Geophysical Research: Space Physics* **114**(A2): A02305.

Heelis, R.A., Sojka, J.J., David, M., Schunk, R.W.:2009, Storm time density enhancements in the middle-latitude dayside ionosphere, *Journal of Geophysical Research: Space Physics* **114**(A3): A03315.

Hudson, M.K., Kress, B.T., Mueller, H-R., Zastrow, J.A., Blake, J.B.:2008, Relationship of the Van Allen radiation belts to solar wind drivers, *Journal of Atmospheric and Solar-Terrestrial Physics* **70**(5): 708–729.

Hudson, M.K.:2012, Where did all the electrons go? *Nature Physics* **8**: 182–183.

Mannucci, A.J., Tsurutani, B.T., Iijima, B.A., Komjathy, A., Saito, A., Gonzalez, W.D., Guarnieri, F.L., Kozyra, J. U., Skoug, R.: 2005, Dayside global ionospheric response to the major interplanetary events of October 29-30, 2003 “Halloween Storms”, *Geophysical Research Letters* **32**(12): L12S02.

Nykiel, G., Zanimonskiy, Y.M., Yampolski, Yu.M., M. Figurski, M.:2017, Efficient Usage of Dense GNSS Networks in Central Europe for the Visualization and Investigation of Ionospheric TEC Variations, *Sensors* **17**(10), 2298.

Perkins, F.:1973, Spread F and ionospheric currents, *Journal of Geophysical Research: Space Physics* **78**(1): 218-226.

Suvorova, A.V., Dmitriev, A.D., Tsai, L.-C., Kunitsyn, V.E., Andreeva, E.S., Nesterov, I.A., Lazutin, L.L.:2013, TEC evidence for near-equatorial energy deposition by 30 keV electrons in the topside ionosphere, *Journal of Geophysical Research: Space Physics* **118**(7): 4672–4695.

Suvorova, A.V., Huang, C.-M., Matsumoto, H., Dmitriev, A.V., Kunitsyn, V.E., Andreeva, E.S., Nesterov, I.A., Tsai, L.-C.:2014, Low-latitude ionospheric effects of energetic electrons during a recurrent magnetic storm, *Journal of Geophysical Research: Space Physics* **119**(11): 9283-9302.

Turner, D.L., Shprits, Yu., Hartinger, M., Angelopoulos, V.:2012, Explaining sudden losses of outer radiation belt electrons during geomagnetic storms, *Nature Physics* **8**: 208–212.

Valladares, C.E., Eccles, J.V., Basu1, Su., Schunk, R.W., Sheehan, R., Pradipta, R., Ruohoniemi, J.M.:2011, The magnetic storms of August 3-4, 2010 and August 5-6, 2011: 1. Ground and space-based observations, *Journal of Geophysical Research: Space Physics* **122**(3): 3487–3499.

Valladares, C.E., Eccles, J.V., Basu, Su., Schunk, R.W., Sheehan, R., Pradipta, R., Ruohoniemi, J.M.:2016, The magnetic storms of August 3-4, 2010 and August 5-6, 2011: 1. Ground and space -based observations, *Journal of Geophysical Research: Space Physics* **122**(3): 3487-3499.

Yizengaw, E., Dyson, P.L., Essex, E.A., Moldwin, M.B.:2005, Ionosphere dynamics over the Southern Hemisphere during the 31 March 2001 severe magnetic storm using multi-instrument measurement data, *Annales Geophysicae* **23**(3): 707–721.

Yizengaw, E., Moldwin, M.B., Dyson, P.L., Fraser, B.J., Morley, S.: 2006, First tomographic image of ionospheric outflows, *Geophysical Research Letters* **33**(20): L20102.